



5-2019

A Bayesian Approach to Multi-Drone Source Localization Methods

Joshua James Gurka

University of Tennessee, jgurka@vols.utk.edu

Follow this and additional works at: https://trace.tennessee.edu/utk_gradthes

Recommended Citation

Gurka, Joshua James, "A Bayesian Approach to Multi-Drone Source Localization Methods. " Master's Thesis, University of Tennessee, 2019.

https://trace.tennessee.edu/utk_gradthes/5453

This Thesis is brought to you for free and open access by the Graduate School at TRACE: Tennessee Research and Creative Exchange. It has been accepted for inclusion in Masters Theses by an authorized administrator of TRACE: Tennessee Research and Creative Exchange. For more information, please contact trace@utk.edu.

To the Graduate Council:

I am submitting herewith a thesis written by Joshua James Gurka entitled "A Bayesian Approach to Multi-Drone Source Localization Methods." I have examined the final electronic copy of this thesis for form and content and recommend that it be accepted in partial fulfillment of the requirements for the degree of Master of Science, with a major in Nuclear Engineering.

Howard Hall, Major Professor

We have read this thesis and recommend its acceptance:

Lawrence Heilbronn, Ronald Pevey

Accepted for the Council:

Dixie L. Thompson

Vice Provost and Dean of the Graduate School

(Original signatures are on file with official student records.)

A Bayesian Approach to Multi-Drone Source Localization Methods

A Thesis Presented for the
Master of Science
Degree
The University of Tennessee, Knoxville

Joshua James Gurka

May 2019

© by Joshua James Gurka, 2019
All Rights Reserved

*I would like to dedicate this paper to two tremendous influences in my life,
James and Johanna Gurka*

Acknowledgements

I would like to express my most sincere gratitude to all of my friends, family, and teachers who have helped me reach this point in my academic career. To Lee Zanger for sparking my interest in the field of nuclear engineering. To my advisor, Howard Hall for providing me an opportunity to further pursue an education and career in nuclear security related work. A special thanks to Matthew Cook for all your support over the years both on and off the SWARM project. Without you none of this would have been possible. Thank you to Kaelyn, Mom, Dad, and Bryan for your endless encouragement and support.

This research would not be possible without the funding provided by the Defense Threat Reduction Agency (DTRA).

Abstract

From abandoned Soviet reactors to lost submarines and stolen medical materials, stewardship of the world's nuclear materials throughout the nuclear age is not what one might hope it to be. The International Atomic Energy Agency (IAEA) estimates around 3000 incidents of illicit trafficking, theft, or loss of radioactive materials have occurred since 1993 [1]. Locating lost or stolen materials is no simple task, particularly when there is little information about the type of source or its activity, whether or not the source is stationary or being transported, and at large distances the signal-to-noise ratio is a limiting factor. Since the USS Scorpion, USS Thresher, and Palomares B-52 searches throughout the 1960's [2], Bayesian inference techniques and Bayesian search methods have become a more commonly embraced approach to complex search missions. The semi-autonomous wide-area radiological measurements (SWARM) system presented in this work utilizes multiple Unmanned Aircraft System (UAS) devices, connected via a central data repository (swarm theory), to more effectively survey a search space and locate missing radioactive sources. Coupling swarm theory with Bayesian inference techniques, SWARM shows great potential in overcoming the challenges of large search spaces and potentially low-count rate contributions from missing radiological sources. Preliminary results prove the search algorithms ability to quickly filter out low probability areas. In simulation, three drones reduced the area of interest by 91.7% after each surveying three lengths of the area at an altitude of 100 meters. The SWARM Bayesian algorithm presented is designed to be a simple and efficient approach to aerial-based Bayesian search localization, applied to a multi-drone search format.

Table of Contents

Chapter 1 Introduction.....	1
1.2 Aerial Search.....	4
1.3 Similar Efforts.....	5
1.3.1 Adaptively Reevaluated Bayesian Localization (ARBL)	5
1.3.2 A Sampling-Based Bayesian Approach for Cooperative Multiagent Online Search with Resource Constraints	7
1.4 Semi-Autonomous Wide Area Radiological Measurements (SWARM).....	7
Chapter 2 Theory	8
2.1 Bayes' Theorem.....	8
2.2 Bayes' Theorem Example.....	10
2.2.1 Early Season Batting Average	10
2.2.2 Monty Hall Problem.....	10
another door. So by updating the conditional probability of a hypothesis with objective knowledge about the situation, a better approximation of the car's true location can be made.	12
2.3 Bayesian Search Methods	12
2.3.1 Bayesian Search Theory.....	12
2.3.2 Maximum Likelihood Estimation (MLE)	12
2.3.3 Nonparametric Density Estimation	14
2.4 Evolution of Applied Bayesian Search Theory.....	15
2.4.1 Palomares H-Bomb	15
2.4.2 USS Scorpion.....	16
2.5 Radiation Counting Statistics.....	16
2.6 Detector Response	17
2.7 Savitzky-Golay Filter.....	18
Chapter 3 Methodology	19
3.1 Search Characterization	19
3.2 SWARM Hardware.....	19
3.3 Algorithm Methodology	20
3.3.1 Code Instantiation	22
3.3.2 Flight Pattern Optimization.....	22
3.3.3 Measurement and Detection Decision	22

3.3.4 Update Probability Search Space	23
3.4 Design Considerations	23
3.4.1 Multithreading	23
3.4.2 Underflow	23
3.4.3 Pandas	24
3.5 MCNP6 Simulation.....	24
3.5.1 Mctal_evaluate.py	26
3.6 Multi-Tier UAS Source Localization.....	26
Chapter 4 Results.....	28
4.1 Multi-Drone Simulation	28
4.2 Multi-Tier Bayesian Localization	36
Chapter 5 Discussion.....	39
Chapter 6 Future Work.....	41
Bibliography	42
Vita	46

List of Tables

Table 1.1: Common Gamma Ray Emitting Radioactive Sources [4]	3
Table 2.1: Conditional probability of a true random selection.	11
Table 2.2: Conditional probability after door A is revealed.	11
Table 3.1: Layout of global dataframe variable.	26
Table 4.1: Rendered x and y coordinates for high-interest areas of Bayesian search at various altitudes..	33
Table 4.2: Rendered x and y coordinates for high-interest areas of non-Bayesian search at various altitudes.....	35
Table 4.3: Rendered high-interest area sizes of Bayesian versus non-Bayesian tests.	35

List of Figures

Figure 1.1: Growth of search area for potential theft from UTK campus [6]	5
Figure 1.2: Log-likelihood results for single and repeated flyovers of a 10 mCi ¹³⁷ Cs source [ARBL].....	6
Figure 2.1: Process flow of Bayesian versus conventional inference techniques	13
Figure 3.1: Process flow of Bayesian search code	21
Figure 3.2: Process flow of Bayesian update process.	21
Figure 3.3: Graphic representation of how data is handled from the individual search agent to the global repository.	25
Figure 3.4: Process flow of Right Angle Turn (RAT) localization method [9]	27
Figure 4.1: X-dimension posterior distributions at search height of 10 meters.	29
Figure 4.2: Y-dimension posterior distributions at search height of 10 meters.	29
Figure 4.3: X-dimension posterior distributions at search height of 50 meters.	30
Figure 4.4: Y-dimension posterior distributions at search height of 50 meters.	30
Figure 4.5: X-dimension posterior distributions at search height of 100 meters.	31
Figure 4.6: Y-dimension posterior distributions at search height of 100 meters.	31
Figure 4.7: Visual representation of high-interest areas from Bayesian search simulation.	33
Figure 4.8: Posterior distribution of surveyed area at 10 meters, no updating.	34
Figure 4.9: Posterior distribution of surveyed area at 50 meters, no updating.	34
Figure 4.10: Posterior distribution of surveyed area at 100 meters, no updating.	35
Figure 4.11: Simulated flight path and resulting prediction from tier 2 search [9].....	37
Figure 4.12: Raw counts and posterior distribution at end of tier 2 search [9].....	37
Figure 4.13: Savitzky-Golay filter over raw data spectrum [9].	38

Chapter 1

Introduction

Dating back to the first and only atomic bombs used by one nation against another, the detonation of “Little Boy” over the Japanese city of Hiroshima and three days later the explosion of “Fat Man” over Nagasaki, the destructive capability of nuclear weapons had been evident to the world. What began as an investigation of neutron-driven chain reactions in heavier elements for prolific electric power generation had quickly become one of the greatest threats facing humanity. Six months following the bombings, at the first general assembly of the United Nations (UN), there was a call for a universal elimination of atomic weapons. However, in the two decades following the first display of nuclear warfare China, France, the United Kingdom, and the Soviet Union would all successfully test nuclear weapons of their own [1]. The nuclear era had arrived, and because the universal surrender of nuclear weapons appeared out of reach, there was an evident need for both domestic and international nonproliferation efforts. As a result, the IAEA was formed in 1957 to encourage the safe use of nuclear materials for scientific and technological advances, while preventing the proliferation of weapons-grade materials to new states [2]. In 1970 the Treaty on the Non-Proliferation of Nuclear Weapons (NPT) was put into effect and today only five states exist as approved weapons states under the NPT; US, Russia, China, UK, and France [3]. Since the 1970’s the list of weapons states has grown from five to as many as nine with non-signatory nations to the NPT [3]. Beyond the use of full-scale nuclear warheads by one of the declared weapons states, the risk of rogue nations or terrorist groups obtaining nuclear materials for use in a “dirty bomb” poses a great challenge to nuclear security, both domestically and internationally [4]. Nuclear materials exist in the industry today for use in a wide range of applications including medical, academic research, commercial power, etc.

Significant resources are put towards properly guarding hazardous radioactive materials in the United States. Theft from a US nuclear reactor is not necessarily the greatest concern with regards to rogue nuclear materials. The more pressing threat arises from countries that do not have the same resources to safeguard their materials properly, or choose not to, creating an

opportunity for theft and smuggling of these sources. An example of a failure to properly protect critical radioactive materials can be observed in the breakup of the Soviet Union. Following the collapse of the Soviet Union in the early 1990's some of the former power's nuclear facilities were abandoned or left insufficiently protected. Today, there potentially exists a nuclear black market throughout the Black Sea region and what is termed a "nuclear highway" through the ex-Soviet states of Georgia, Armenia, and Azerbaijan. This nuclear highway provides trade routes for these unaccounted-for radioactive sources into ISIS controlled regions of Syria and Iraq [5]. Multiple interceptions of these trade attempts in the last decade have in fact linked the confiscated Uranium to that used in Russian reactors [5]. A substantial amount of former Soviet nuclear fuel is still unaccounted for [5]. Not only is the location of these materials a mystery, but it is unknown exactly how much is out there.

A critical mass of a weapons-usable isotope such as U-235 or Pu-239 isn't necessary to induce a radiological disaster; rather, any amount of highly radioactive material can be detonated and dispersed throughout a highly populated urban area, with the use of conventional explosives, thereby causing radiation poisoning for unsuspecting bystanders as well as lasting economic effects. In such a situation, decontamination of the affected area alone would be a lengthy and expensive process. This is known as a dirty bomb. Nuclear bombs are considered Weapons of Mass Destruction (WMD) but dirty bombs are Weapons of Mass Disruption where, contamination and widespread public anxiety are the primary goals of the adversary [4].

Dirty bombs exist in two main forms; Radiological Dispersal Devices (RDD) and Radiological Exposure Devices (RED). RDD's combine radioactive material with conventional explosives to contaminate the surrounding area with radioactive material. RED's simply conceal radioactive material in a crowded area, for example, a source in a backpack on a bus or in the crowd of a concert, intended to deliver high doses to people nearby, and potentially cause acute radiation sickness. Gamma rays are deeply penetrating, thus strong gamma emitting sources are a significant concern for both RDD's and RED's. Table 1.1 shows some commonly encountered gamma sources that could be obtained and used in a dirty bomb attack.

As industrial use of nuclear materials continues to increase, the problem of keeping these materials secure becomes exponentially more difficult. It is estimated that over one hundred incidents of theft or loss of these materials occur per year leaving thousands of rogue sources scattered around the world [5].

Table 1.1: Common Gamma Ray Emitting Radioactive Sources [4]

Isotope	Use	Minimum Activity (Ci)
Cs-137	Industrial Sterilization	5000
	Medical Sterilization	1500
	Nuclear Medicine	5
Co-60	Industrial Sterilization	5000
	Medical Sterilization	1500
	Industrial Radiography	11
Ir-192	Industrial Radiography	5
	Nuclear Medicine	0.02

Dirty bombs are not intended to destroy so much as they are intended to spread fear. While the physical damage and cleanup is a major concern, should a dirty bomb be used, the resulting psychological effects and public distress are much longer lasting concerns. It is essential that the US continue its efforts aimed at preventing these devastating attacks before they can come to fruition, by more effectively locating lost or stolen radiological sources. The research presented utilizes aerial search agents with Bayesian inference techniques to address this critical security need.

1.1 Past Efforts

The SWARM project is a follow up effort extending off the work done first by Dr. Samuel Willmon and then by Blake Wilkerson on the Broad Area Search Bayesian Processor (BASBP) project. Dr. Willmon originally looked into utilizing Bayesian processing techniques to improve the signal-to-noise ratio in aerial detection systems. The original theory for the BASBP project can be found in his dissertation [7]. Blake Wilkerson was responsible for taking Dr. Willmon's original theory and developing it into a working algorithm to operate in conjunction with a detector system and geographical data to eliminate low or zero-chance areas and locate radioactive sources within a search space [4]. Mr. Wilkerson's algorithm was built to operate

with one search agent, and ran in conjunction with the Monte Carlo N-Particle (MCNP6) transport code to simulate flux data and subsequent detector response for a known source at a given distance from the detector.

1.2 Aerial Search

When searching for misplaced or stolen radioactive materials, factors such as the source strength, signal-to-noise ratio (SNR), and potential shielding of the source can make search methods more difficult. Ground-based search methods are limited by resources and the accessibility of the vehicles in the terrain to be searched. Additionally, after theft there exists a time-distance relationship that is of significant concern, as illustrated in Figure 1.

A more effective approach to locating these orphan materials is to deploy unmanned aircraft systems (UAS) to the search space. Drones can cover large areas of interest more effectively than a human and can search areas unreachable by ground vehicles. Using aerial search agents also prevents sending humans into potentially hazardous situations.

While aerial search methods show significant upside to the ground-based alternative, they do come with their own set of complications. As previously mentioned, SNR poses a major complication to aerial-based detection systems as the strength of the source falls off by the square of the distance from the detector. Since drones will normally be operating from relatively far working distances, the detection limits of the system are an inhibiting factor.

In most scenarios, varying background signals can affect detection statistics. This issue is of particular concern in large urban environments where background radiation varies spatially. Large buildings, and other man-made obstacles can have contributing radiation effects to the gross measurements of the detector.

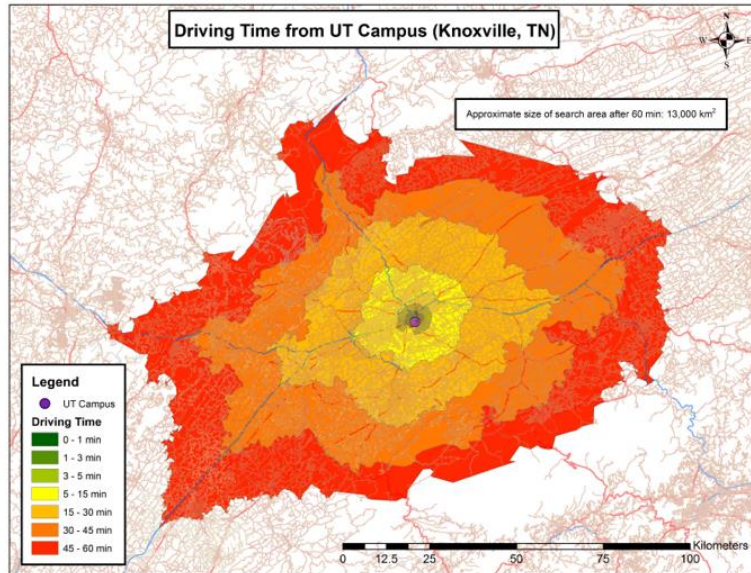


Figure 1.1: Growth of search area for potential theft from UTK campus [6]

In his thesis, Blake Wilkerson showed the ability of the Bayesian framework within the BASBP project to improve localization of sources weaker than standard minimum detectable activities [4]. Deploying multiple drones to a search space drastically increases the amount of data that can be obtained as well as the area that can be covered in the same amount of time. More data improves the confidence in the Bayesian estimate of a sources location within the search space. Thus, by increasing the number of drones actively surveying the area, the SWARM effort presented in this report aims to take aerial-based source detection methods beyond their current elementary state and bring multi-drone source localization to fruition.

1.3 Similar Efforts

1.3.1 Adaptively Reevaluated Bayesian Localization (ARBL)

This effort based out of Pacific Northwest National Lab (PNNL) presents a novel Bayesian approach to aerial localization of radiological sources in urban or rural environments. They use an arbitrarily complex directional detector along with local topography information and corresponding background radiation data. Then a Maximum Likelihood Estimation (MLE) approach (see Section 2.3.2) is employed, by comparing incoming data against a library of

precalculated detector responses, to various sources at a given location and distance from the detector, to locate sources in real-time and update the likelihood function mapping.

This project performs multiple one-dimensional flyovers spanning multiple kilometers throughout a simulation. To account for the computational issues associated with limited field of view measurement redundancies (i.e. points near the center being measured more repeatedly than points near the outside, which can drive down the likelihoods of the heavily-measured regions) the group uses a likelihood ratio test as a normalization factor.

The one-dimensional flight paths resulted in significant lateral uncertainty. Repeated flyovers showed improved uncertainty levels as seen in Figure 1.2. The second flyover showed a more distinct point of interest near the sources location (at the origin). Results of the ARBL tests were able to find sources within 20 meters of the true location.

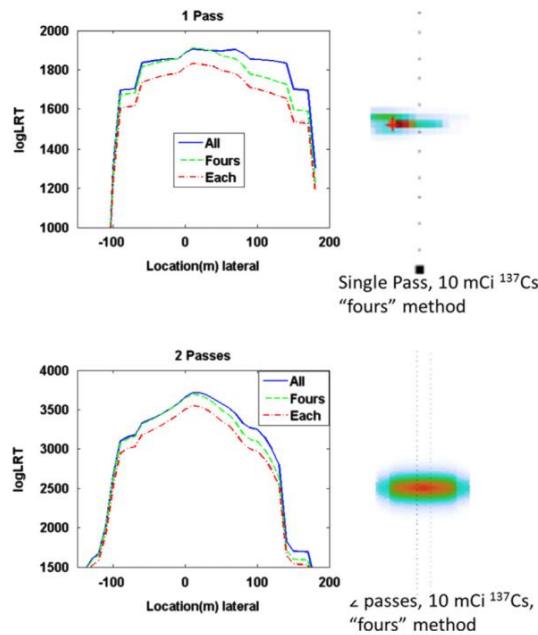


Figure 1.2: Log-likelihood results for single and repeated flyovers of a 10 mCi ^{137}Cs source [ARBL]

1.3.2 A Sampling-Based Bayesian Approach for Cooperative Multiagent Online Search with Resource Constraints

Hu Xiao et. al. present a Bayesian framework for multiagent search of a target on a 2-D plane. The Bayesian framework works similarly to the SWARM effort presented in this report; updating local probability density functions of the target as search agents obtain new information. However, Xiao utilizes particle sampling methods and a Gaussian mixture model (GMM) to create the global PDFs which are then used to make estimations regarding local parameters [8]. The SWARM project makes global assertions based on the collective local observations.

1.4 Semi-Autonomous Wide Area Radiological Measurements (SWARM)

This research aims to advance the current state of aerial search methods by utilizing multiple search agents in conjunction with Bayesian inference techniques to effectively locate a radiological source within a search space. The various search agents will operate as instances of the the algorithms class structure, feeding data to a central repository where it can be compiled and used to update the belief in the source(s) location. The SWARM effort will use a maximum likelihood estimation (MLE) technique to estimate and account for background radiation levels in real time, and a Bayesian search algorithm, with no prior knowledge or data library, to locate a source(s) of unknown identity or strength. The aim is to design an algorithm that is both efficient and versatile so that it can rapidly locate any source of interest with little to no prior knowledge.

Building off of the BASBP effort, which focused on incorporating geographical data to eliminate low probability areas, the SWARM project intends to locate the target source within a region by iteratively reducing the search area based on the likelihood of the source's location within the space.

Chapter 2

Theory

The SWARM project relies heavily on Bayesian inference techniques to locate illicit materials and rogue sources. This chapter will outline the essential background information and theoretical principles of Bayes' theorem, as well as examples to demonstrate the versatility and application of Bayesian search and inference methods.

2.1 Bayes' Theorem

Bayes' theorem is named after the renowned 18th century mathematician Thomas Bayes. Bayes originally conceptualized the theorem as a way to make rational conclusions about the existence of God based on observations in the world around him [8]. This early application is important to understand when considering the intention of Bayes' theorem; despite its widespread use in statistical and mathematical models, Bayes' theorem is a measure of belief in a hypothesis, not a statistical certainty. Bayes never published his discovery, instead it was posthumously presented to a London group of intellectuals by Richard Price [8]. In his unpublished manuscript, Bayes focused specifically on easy to compute probabilities to update prior assumptions with objective evidence from repeatable experiments in order to make assertions about the world around him. He never put these concepts into a formal equation. The modern mathematical form and scientific application of Bayes' theorem (equation 2.1) is credited to Pierre-Simon Laplace.

$$P(A|B) = \frac{P(B|A) * P(A)}{P(B)} \quad (2.1)$$

Where, $P(A)$ is the *prior* estimate, the initial estimate of belief in a given hypothesis.

$P(B|A)$ is the *likelihood* estimate, the probability of each new piece of information under the given hypothesis.

$P(B)$ is a normalizing factor, the probability of the data in all possible scenarios.

$P(A|B)$ is the *posterior* estimate, the updated probability of the hypothesis (against the data collected).

Throughout the late 18th and early 19th centuries, Bayes' theorem was met with controversy over the assertion that it was simply quantifying ignorance. Since then the revolutionary equation has allowed mathematicians and scientists, to tackle some of the world's most complicated questions by taking an initial belief, updating it with a wealth of data and new knowledge, and postulating a most probable solution [2]. Thanks to Bayes' theorem, Alan Turing was able to crack the German enigma codes, the United States Navy was able to locate missing submarines, H-bombs, and scientists were even able to predict the Challenger shuttle disaster [2, 6].

By Bayes theorem the posterior estimate is updated as new data is available to form a likelihood estimate and weight against the prior. This update is normalized by the probability of all scenarios, $P(B)$, where,

$$P(B) = \int P(B|A) \cdot P(A) dA \quad (2.2)$$

For the prior, likelihood, and posterior estimates, an exact probability is not required for Bayesian inference methods. Values related to the probability such as a probability density can be used to represent the relative belief in one hypothesis over another. Within this project probability densities are utilized to express the confidence of a source's location in a search space.

There are multiple schools of thought when it comes to determining an effective prior estimate. The first is to assign an even probability to all hypothesis, this is known as a zero-bias prior. The alternative is to insert bias and more heavily weight a certain hypothesis before collecting any objective data. In more complex scenarios such as searching a large area for rogue radioactive material, certain areas can be ruled out as improbable based on prior knowledge. For example, a source is most likely not located in the middle of a body of water when it is known that the adversary is travelling by car. Aside from objective knowledge to rule out low or zero-probability areas, inserting bias into a prior estimate can wrongly skew the posterior distribution when initial data is collected, and take longer to reflect an accurate belief in the hypothesis.

The key concept to take from equation 2.1 is that the posterior is proportional to the prior times the likelihood. To improve the posterior distribution, one either needs a more accurate prior or more data to weight the distribution by. Since often there is no knowledge to begin with a more informed prior, more data is needed for a better posterior distribution.

Bayesian search methods work in an iterative fashion, updating the posterior each time new data is available. Assuming a source is indeed within the search space, each piece of new information is valuable because even not finding a source in a specific area increases our confidence in the other locations. After each update the posterior estimate can be recycled as an informed prior estimate for the following iteration.

2.2 Bayes' Theorem Example

2.2.1 Early Season Batting Average

A simple example to demonstrate the key concepts behind Bayesian inference is to consider the problem of estimating a player's batting average for the season before the season starts. A safe assumption is the player will hit somewhere between 0.210 and 0.350 on the season so 0.270 will serve as the prior estimate. This can be represented as a β -distribution with parameters $\alpha = \text{hits}$ and $\beta = \text{non-hits}$.

$$\text{Batting Avg.} = 0.270 = \frac{\alpha}{\alpha + \beta} = \frac{81}{81 + 219}$$

If after 300 at-bats the player has 100 hits, we can update the posterior estimation of the player's season long batting average to reflect the new information available:

$$\text{Batting Avg.} = \frac{81 + 100}{(81 + 100) + (219 + 200)} = 0.303$$

The player hit 0.333 through his first 300 at-bats, which is a hall-of-fame caliber batting average. It is unlikely he would sustain that average throughout the season. Thus, weighting the data against a prior estimate helps protect the overall posterior estimate from fluctuations or outliers.

2.2.2 Monty Hall Problem

Another classic problem that is commonly associated with Bayes' theorem, and will assist in introducing the idea of conditional probabilities, is the Monty Hall problem. Consider you are on

a game show and there are three doors, labeled A, B, and C. Behind one door is a brand new car and behind the other two are goats. So, initially there is a $1/3$ chance of the car being behind any door. You select door B, but before the host reveals what is behind door B he opens door A to reveal a goat and asks you if you'd like to change your pick. Is it better to switch, stay with your original pick, or does it not matter? Bayes' theorem shows us that it is always better to switch.

If the host were to pick any door to reveal, the process would be random and we could represent the probability of the car being behind door A (the revealed door) and door B (the selected door) by Table 2.1. However the door the host selects to reveal is not random because the host knows which door the car is behind and will never select that door. Thus the probability of the car being behind door A is zero and in order to keep the total probability equal to 1, the $1/3$ probability of $(A \cap \sim B)$ is pushed to $P(\sim A \cap \sim B)$. After the host opens door A to reveal a goat, the game probabilities shift to the values laid out in Table 2.2.

From the Bayesian standpoint, the probability of the car being behind the original selection, once one of the possible doors is removed, is less than the probability that it is behind

Table 2.1: Conditional probability of a true random selection.

	P(A)	P($\sim A$)	Total
P(B)	0	$1/3$	$1/3$
P($\sim B$)	$1/3$	$1/3$	$2/3$
Total	$1/3$	$2/3$	1

Table 2.2: Conditional probability after door A is revealed.

	P(A)	P($\sim A$)	Total
P(B)	0	$1/3$	$1/3$
P($\sim B$)	0	$2/3$	$2/3$
Total	0	1	1

another door. So by updating the conditional probability of a hypothesis with objective knowledge about the situation, a better approximation of the car's true location can be made.

2.3 Bayesian Search Methods

2.3.1 Bayesian Search Theory

Bayesian search methods have been employed by the military for a number of challenges, dating back to World War II, despite the reluctance to admit it. Perhaps the most famous implementation of Bayesian inference techniques during WWII was Alan Turing cracking the German Enigma codes [2]. During the Cold War the military used the same search methods to locate missing Soviet and American submarines [2] as well as the missing hydrogen bomb off the coast of Palomares, Spain [7].

The underlying approach of Bayesian search methods is to:

1. Outline all possible hypothesis regarding the location of the search target.
2. Assign a *prior* probability to each hypothesis.
3. Determine the *likelihood* of detecting the search target if it is there.
4. Update the *prior* hypothesis with objective data from the search to determine the new probabilities of each hypothesis, known as the *posterior*.

Figure 2.1 depicts the primary difference between Bayesian and frequentist inference methods. Frequentist methods are normally less computationally intensive and start with parameters for the statistical model in order to make assumptions about both observed and unobserved data. Bayesian inference, on the other hand, incorporates prior knowledge with the calculated likelihood of data observed to make a hypothesis about the parameters of the problem. Where, μ is the mean value and σ is the standard deviation of the data.

2.3.2 Maximum Likelihood Estimation (MLE)

Maximum likelihood estimation is a method to find the parameters of a model by means of maximizing the likelihood of the parameters against the data observed. In context, this project

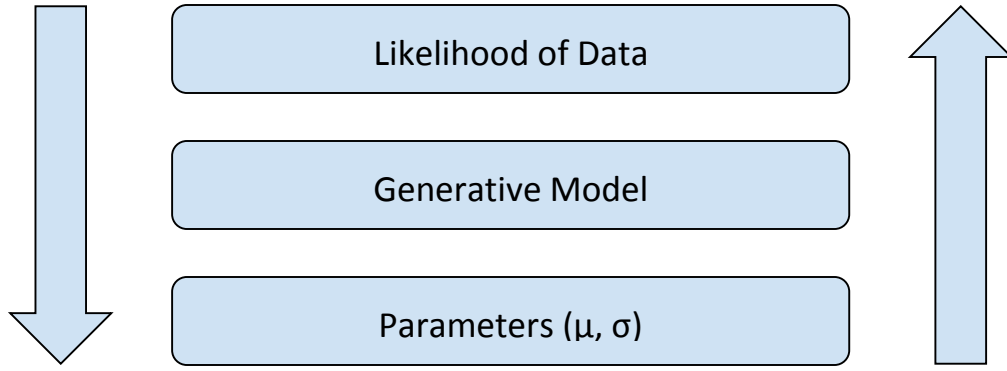


Figure 2.1: Process flow of Bayesian versus conventional inference techniques

aims to determine background radiation levels, of a search space, in real-time. For complex urban areas background radiation levels can vary drastically. Thus a simple background calibration measurement at one point in the space would not be an accurate estimation of the average background radiation throughout the entire area of interest. Using MLE to update the likelihood of the mean background radiation counts as data is acquired is an efficient way to account for background radiation without a-priori knowledge of the landscape.

Equation 2.3.1 is the probability density of an observed data point against a Gaussian model with parameters μ and σ .

$$P(x; \mu, \sigma) = \frac{1}{\sigma\sqrt{2\pi}} \exp\left(-\frac{(x-\mu)^2}{2\sigma^2}\right) \quad (2.3.1)$$

For computational reasons we will take the log transform of this function and work with the log probability density function (pdf). For more information on this see Section 3.4.2. Equation 2.3.2 shows the log probability density of the observed data point against the predicted model

$$\ln(P(x; \mu, \sigma)) = \ln\left(\frac{1}{\sigma\sqrt{2\pi}}\right) - \frac{(x-\mu)^2}{2\sigma^2} \quad (2.3.2)$$

And the total log-likelihood of an entire dataset X can be calculated from

$$\ln(P(X; \mu, \sigma)) = \ln\left(\frac{1}{\sigma\sqrt{2\pi}}\right) - \sum_n \frac{(x-\mu)^2}{2\sigma^2} \quad (2.3.3)$$

In order to find the maximum likelihood for the parameter μ take the partial derivative of equation 2.3.3 with respect to μ and solve. This works out to be

$$\frac{\delta \ln(P(X; \mu, \sigma))}{\delta \mu} = \frac{1}{\sigma^2} (\sum_n x - n\mu) \quad (2.3.4)$$

Setting equation 2.3.4 to zero and solving for μ will return the highest likelihood value for the data observed. This value can be updated as more data becomes available to maintain as accurate of an approximation of the average background radiation levels according to the information available.

MLE is a powerful tool for aerial search projects. However, it does not offer the same capability as Bayesian inference methods to insert prior knowledge. MLE will strictly be used in estimating the average background radiation levels of the area. From there, Bayesian inference methods will take over in estimating the source(s) location.

The key difference between Bayesian inference and MLE methods is that MLE calculations treat the parameter of interest as a point estimation, while Bayesian methods treat it as a random variable.

2.3.3 Nonparametric Density Estimation

Nonparametric density estimations do not operate under the assumption that the data will follow a specific model like parametric estimations do (i.e. Normal or Beta distributions). This is beneficial for circumstances where anomalies can potentially create non-smooth distributions and skew the parameter estimations. Within the scope of this project, large urban areas or multiple sources present in the search space will make it difficult to fit the data to a particular parametric model. Nonparametric density estimations, such as a Kernel Density Estimation (KDE), offer a potentially effective method for calculating the probability density function of a random variable in complex problems such as source localization.

2.4 Evolution of Applied Bayesian Search Theory

2.4.1 Palomares H-Bomb

In January of 1966 a B-52 bomber was enroute from North Carolina to Europe when a miscommunication between the bomber pilot and the pilot of a KC-135 refueling aircraft caused both planes to go down over the coast of Spain. The bomber was carrying four Mk28-type hydrogen bombs. One bomb was recovered intact, two of the bombs' cores were destroyed and scattered over surrounding farmland, and one of the bombs was nearly 3000 feet deep in the ocean.

After weeks of no success locating the missing bomb, the Air Force finally asked the Navy for assistance. The U.S. Navy brought on John Craven, a proven expert in problems such as this. Craven successfully located the U.S.S. Thresher in 1963 and the U.S.S. Scorpion a few years after the Palomares search (1968) [2] (see Section 2.4.2).

Craven and his team explored a number of possible outcomes for the bomb's descent based on how many parachutes may have deployed, if it remained intact, etc. They then placed bets on the most likely scenarios and applied probabilities to each. This produced the first likelihood map with seven locations of interest. When the original search of these locations turned up empty, the likelihood map was updated.

A fisherman named Francisco Orts had originally reported the location of the missing bomb to the Air Force, at the beginning of the search, but his testimony was disregarded because he did not use what the Air Force deemed appropriate methods to note the location where the bomb landed. After Craven took over, he tracked down Orts, asked him to show where he thought the bomb had descended, then drew a mile radius around that location and named it "Alpha I" [2]. The bomb was eventually located within a mile of Orts' pinpoint. Dr. Henry Richardson used Bayes' theorem to calculate the value of Orts' testimony and it was determined that his account saved the government at least a year's worth of effort [2].

Finding the missing bomb off the coast of Palomares, Spain, across hundreds of square miles of poorly-mapped ocean floor, when the only information regarding its location was a local fisherman's account from afar, was no simple task. Bayesian search methods proved to be a powerful tool for difficult search problems such as this.

2.4.2 USS Scorpion

In May 1968, shortly after the Soviet submarine K-129 went missing, the USS Scorpion was reported missing when it failed to make port in Norfolk, Virginia. The submarine was on a 3,000-mile route from Spain to Virginia and no distress signals were received to indicate a potential problem on board. Fortunately, an unnamed agency monitoring radar and sensor data was able to localize an unusual event about 400 miles off the coast of the Azores, which corresponded with the anticipated path of Scorpion [2]. This bit of information narrowed the search space from a 3000-mile-long area to roughly a few square miles [8]. Still, locating a missing submarine in roughly 4 square miles of ocean stretching to depths greater than 2 miles is no simple task. The primary difference between the Palomares H-bomb search and the search for the USS Scorpion was that the Palomares search did not utilize Bayesian priors in combination with search effectiveness probabilities (SEP). For this search a powerful computer back in the United States would compute the probabilities of the pre-search hypothesis, then these priors were combined and updated on the ship with the daily results of the search. Treating the search space as a standard Euclidean 2-space X , with coordinates designated by ordered pairs (x_1, x_2) , where x_1 and x_2 are independent, normally distributed variables with mean 0 and standard deviations σ_1 and σ_2 , respectively, the probability density function for the location of the missing ship can be modeled by:

$$p(x_1, x_2) = \frac{1}{2\pi\sigma_1\sigma_2} \exp\left[-\frac{1}{2}\left(\frac{x_1^2}{\sigma_1^2} + \frac{x_2^2}{\sigma_2^2}\right)\right] \quad \text{for } (x_1, x_2) \in X \quad (2.3.5)$$

The problem of finding a missing submarine was then at least simplified to finding a stationary target with a bivariate normal distribution. The remnants of the USS Scorpion were found on October 30th, 1968 [2].

2.5 Radiation Counting Statistics

The general theory for particle flux, at distance r , from a point source is given by equation 2.3.

$$\phi = \frac{S_0}{4\pi r^2} e^{-\mu x} \quad (2.3)$$

Where ϕ is the radiative flux,
 S_0 is the source strength,
 μ is the attenuation coefficient of the shielding material, and
 x is the depth of shielding.

From equation 2.3 it can be seen that the flux falls off by r^2 . While the expected signal drops off exponentially as a detector moves away from a source's location, radiation counting statistics (i.e. the number of photons hitting a detector in a given interval) follow a type of normal distribution known as a Poisson distribution. This relationship is fundamental for the calculations involved in this project. An exponential falloff hinders the detection capability at far-off detection distances. Additionally, the $1/r^2$ dependence makes detection in areas of already low signal-to-noise ratios difficult. Thus any signals above background levels become potential areas of interest.

Unlike this project's predecessor (BASBP), SWARM will not use the flux data from a Monte Carlo transport code to weight particles around a measurement's location. The objective of this project is to be able to locate missing sources of unknown composition and strength. Tools like Monte Carlo N-Particle (MCNP6) rely on source information (i.e. composition, strength, location) to model particle data and subsequent detector response at all points within the search space. For SWARM measurements of raw counts, along with simple particle flux theory principles, are used to determine the likelihood probabilities within the area of interest.

2.6 Detector Response

The detection system response involves both the physical response from the interaction of radioactive material with the detector material as well as the response of the electronics. This project utilizes plastic scintillators onboard each UAS. Scintillation detection can be summarized by two broad steps:

1. Absorption of energy from incident radiation in the scintillation material and subsequent emission of photons.
2. Amplification of the light and production of an output signal. [16]

Thus scintillation detection relies heavily on how effectively incident radiation deposits energy.

2.7 Savitzky-Golay Filter

The Savitzky-Golay filter is a data smoothing function that helps boost signal-to-noise ratios without drastically distorting the data. It utilizes a linear least-squares method to fit low-degree polynomials to a series of adjacent data points otherwise known as convolution [SG wiki].

Convolution methods define two functions from adjacent data series, and then a third function to model how a change in one of the fits modifies the other. This enables larger differentials over shorter distances to be distinguished from background noise, increasing the ease, and accuracy of hotspot identification.

Chapter 3

Methodology

The objective of the SWARM project is to be able to deploy multiple UAS devices and return the posterior probability about the lost or stolen source's location from a distributed detection network, in a computationally time-efficient manner. This chapter outlines the problem statement for the SWARM project and explains the various approaches and considerations taken in designing and implementing this novel algorithm.

3.1 Search Characterization

Source detection is a broad topic with far more ways to complicate the problem than to simplify it. When addressing such complex problems it is essential to keep the scope of the investigation within reason. In designing the Bayesian algorithm the following assumptions were applied:

The source(s) is stationary throughout the search.

The source(s) is within the defined search space (i.e. $P(B) = 1$).

The activity and specific nuclide is unknown.

Gamma flux is independent of the UAS' velocity.

No prior knowledge of background radiation levels is available.

Non-directional detector is used for the search.

By assuming there is no prior knowledge about the source (i.e. strength, identity), and thus not comparing the obtained data against a precalculated library, the intention is that the search algorithm has the versatility to be used in a wider range of scenarios beyond the immediate scope of this effort.

3.2 SWARM Hardware

For live implementations of the Bayesian algorithm this project will utilize Pixhawk flight-controlled quadcopter UAV. There are currently two HSE AG6 UAVs for live deployment, with

a third to be bought in Fall 2019. The radiation detection system on board will consist of an Eljin plastic scintillator, a Bridgeport Instruments USB base, and a linear focused photomultiplier tube (PMT). For the time being a Raspberry Pi or Linux OS-based Laptop will be used in conjunction with a compatible camera for spectral imaging purposes, with the hope of upgrading to a BaySpec OCIM Push Broom Multispectral Imaging Camera run with Windows 7 PRO on a mini-computer. The computations onboard will be made by a Linux-based OS computer system. In addition to the onboard detection and computation systems, communications to and from the UAS will rely on XBee radios operating at 900 MHz. This operating frequency will allow the UAS to transmit data from greater distances, but at the expense of a lower bit rate. Standard serial communications will be used to communicate between the associated computer and the XBee radio attached along with any other external hardware (such as GPS units).

3.3 Algorithm Methodology

At its core the Bayesian algorithm design follows a rather simple outline, guided by the Bayesian concepts explained in Chapter 2. It combines prior knowledge with incoming data to update the probability space. The process flow of the Bayesian code is depicted in Figure 3.1. The Bayesian code was designed in Python because of its object-oriented capability and subsequent flexibility with handling large and complex data structures. All functionality of the Bayesian code is self-contained in a class structure to enable it to be either passed or overwritten through a proper class inheritance structure. This organization of the code is intended to reduce redundancy within the project as well as keep the code as simple, robust, and flexible as possible for future iterations to build off with minimal difficulty. The aim of this project is to remain platform and source agnostic. The class structure of the Bayesian algorithm allows for more specific designations of the code to recycle all core functionality and tailor individual class attributes and methods to the parameters of the search.

Figure 3.2 displays the iterative process flow of the Bayesian algorithm update method. The dotted line outlining the arrow from the *Initial Prior* to the *Global Data Repository* is to signify that this process only occurs once, at the initialization of the search. Since no data is present at the start, an evenly weighted prior distribution will serve as an unbiased prior hypothesis. Beyond the initial calculation of the likelihood of the data against the prior hypothesis, the resulting posterior distribution is recycled as an educated prior for future updates.

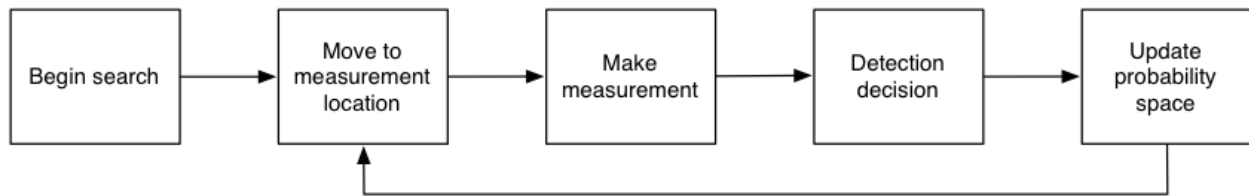


Figure 3.1: Process flow of Bayesian search code

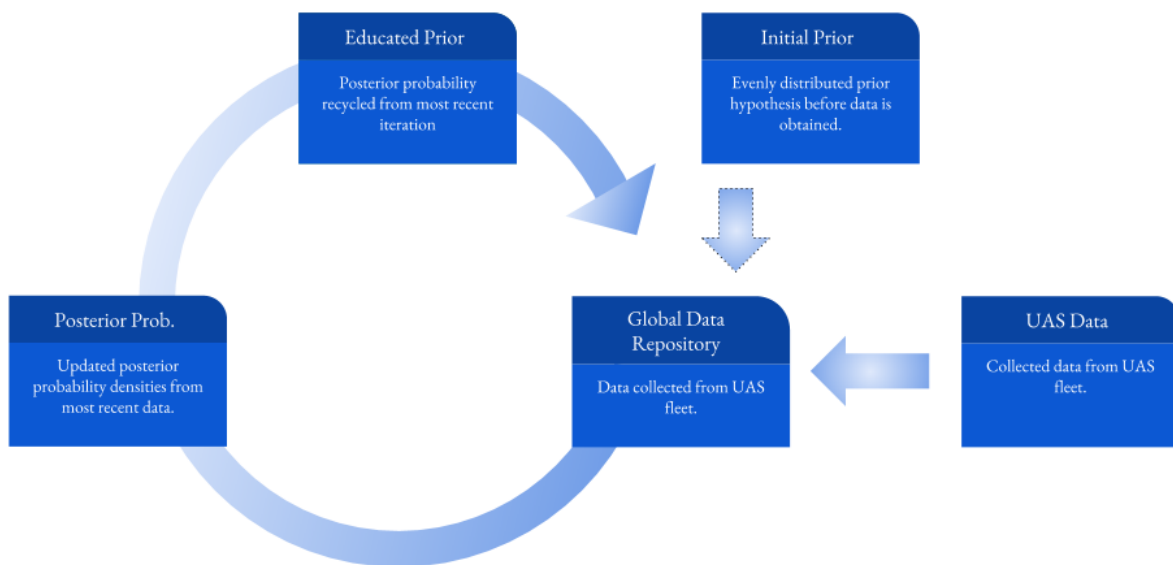


Figure 3.2: Process flow of Bayesian update process.

The data collected by the UAS fleet, along with the prior and posterior distributions, is stored in a global data repository. From this update process a visual of the most current posterior distribution is rendered for the user.

3.3.1 Code Instantiation

The SWARM Bayesian search program can be initiated by running the `Swarm.py` file. This program begins by prompting the user for the number of drones in the swarm. From this the program will create as many instances of the Bayesian class. An instantiation of the Bayesian class will then create a dataframe, as an attribute of the instance, for a drone to feed data back to. All instance dataframes will feed into a central repository, which the main script of the Bayesian class is programmed to use for updating the posterior distribution.

3.3.2 Flight Pattern Optimization

Flight patterns are predetermined in the large and medium area search efforts to locate radiological hot spots. Based on the highlighted areas determined by these initial surveys of the search space, a local Right Angle Turn (RAT) method (see Section 3.5) will be used to autonomously pinpoint a more exact location.

3.3.3 Measurement and Detection Decision

Within the simulation tests, a measurement is represented by extracting a data point from a location along the search agent's path and adding it to the global data repository. In live flights the detectors onboard the drones will continuously stream data (count rate, latitude, longitude, and altitude) to the onboard computer.

Visual rendering of the resulting posterior distribution as the area is surveyed will allow for basic user hotspot identification. To better distinguish the maxima within the data, a Savitzky-Golay filter will be applied (see Section 2.6). Methods within the Bayesian class allow the user to set a desired confidence threshold, above background levels, to label a local maxima as a hotspot and begin the RAT pinpointing method (see Section 3.5)

3.3.4 Update Probability Search Space

A distinguishing feature of Bayesian inference techniques is the incorporation of prior knowledge, weighted against incoming data, to update the posterior hypothesis. Since the Bayesian algorithm calculates the probability densities under a log transform, the likelihood and prior probability densities are summed each update (as opposed to multiplied, by eqn. 3.1). This posterior distribution is recycled as the next prior hypothesis before it is brought out of the log transform and normalized for the rendered graphic representation. The probability density values under the log transform are not normalized. Thus, creating an inherent weighting factor as newly calculated likelihoods are added and probability density values accumulate each update. A basic process flow of the Bayesian update method can be seen in Figure 3.2.

3.4 Design Considerations

While the primary focus of this project is to search for and locate rogue radioactive sources, it is impossible to anticipate the exact scenario. Thus, the intent is to design the code such that it is versatile in application, as well as detector and platform agnostic. In addition, the code must be designed such that it can efficiently handle large amounts of data, streaming from multiple search agents simultaneously.

3.4.1 Multithreading

In an effort to allow for receiving and transmitting signals simultaneously between the ground station and n-number of UAS agents, multithreading capability was integrated into the code. Without multiple threads running, the code would have to wait on the information to be transmitted, or received, before processing another transmission. Additional threads, however, allow for asynchronous tasks to run in the background and prevent potentially losing data or delayed commands to the drone due to backed up communication channels. Threading functionality is inherited from the class threading within python's standard library.

3.4.2 Underflow

The hypothesized location of the source within the search space is represented using probability densities. By equation 2.1 the prior and likelihood probabilities are multiplied, then divided by a normalizing constant. When working with large datasets the probability densities tend to be very

small, near-zero values. Multiplying several small decimal values eventually results in python rounding down to zero, and the distribution is lost. This is known as underflow. To counter this issue the Bayesian code processes the update of the posterior distribution under a log transform so the prior and likelihood probability density values can be added and subtracted instead of multiplied and divided. Addition and subtraction is also less computationally taxing than multiplication and division, allowing for the code to process updates faster. This difference in computation time is minimal, however more noticeable as the amount of data increases. As previously mentioned, the objective is to design the Bayesian code to be as robust as possible in order to handle larger scale areas and more complex problems than the scope of this project encompasses, in future extensions of this work. Thus even incremental improvements to the code's speed is of value.

3.4.3 Pandas

Data within the Bayesian algorithm is contained and manipulated inside pandas dataframes. All functionality and operations of the Bayesian code could be designed using core Python packages. However, packages such as pandas and numpy offer extensive advantages for more complex data structures and data analysis. Pandas is a wrapper for numpy functionality with added flexibility with regards to organizing and indexing data. Tests within the scope of this effort read in data as an array. The flexibility added from incorporating the pandas library allows the algorithm to handle input data in other forms, such as a string or dictionary, with minimal change to the code.

3.5 MCNP6 Simulation

Prior to employing the Bayesian algorithm in the field, a simulated environment was created using MCNP6 to allow the Bayesian code to be tested, and adjusted as needed, for a single source scenario. An F4 tally, which models the average particle flux across a cell, was used to create simulated data.

The energy deposited at a given point in the simulated environment represents a single measurement by a search agent. Methods within the Bayesian class can take multiple points along a predetermined, or random path to simulate multiple agents taking measurements at once.

Figure 3.3 displays how multiple drones, represented as instances of the UAS class, a subclass inheriting from the Bayesian class, can simulate taking measurements within the search

space, by taking sample data points from a precalculated MCNP tally, and feeding that data back to the global repository. This global dataframe is what is passed to the Bayesian processing methods of the code. It instantiates as an array of equal nonzero values to provide an unbiased prior before any data is obtained. As the data is fed from the search agents it overwrites the previous data point.

Data is collected and stored as (1x4) arrays with columns: Value, Latitude, Longitude, and Altitude. After calculating the likelihood distribution a column is added containing the log probability density values. By the end of the Bayesian processing methods the central dataframe layout resembles Table 3.1

The Log PDF column serves as the likelihood of the collected data and is recalculated each time new data is obtained and added to the dataframe. For the Update() method the Log PDF and Prior columns are used in calculating the posterior distribution. The Update() method is designed to first check if a Prior column exists. If it does not, that means it is the first iteration of the Bayesian process and it simply passes the likelihood values as the posterior because there is no prior calculation to weight the values against. In all subsequent updates the prior and likelihood values are both used in determining the posterior hypothesis values. For either case, the posterior values are then recycled and stored as the prior hypothesis for the following update calculation.

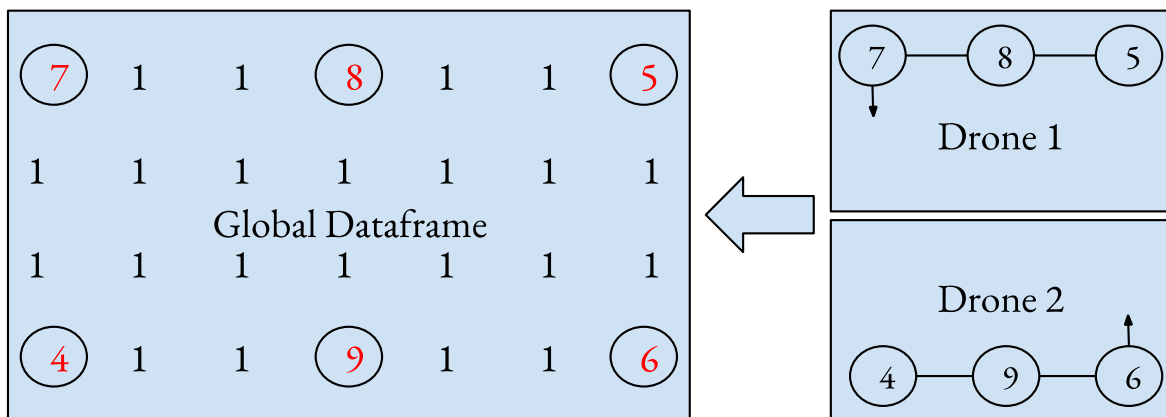


Figure 3.3: Graphic representation of how data is handled from the individual search agent to the global repository.

Table 3.1: Layout of global dataframe variable.

Value (Unit)	Latitude (Degrees)	Longitude (Degrees)	Altitude (m)	Log PDF	Prior	Posterior
51	35.9544	83.9295	50.1	-7.025	-5.551	-12.576
55	35.9550	83.9285	52.0	-6.454	-7.380	-13.934
40	35.9552	83.9281	51.5	-8.721	-10.252	-18.973
47	35.9559	83.9269	50.8	-6.903	-5.649	-12.552

3.5.1 Mctal_evaluate.py

MCNP6 returns tallys as a mctal file. Mctal_evaluate.py, developed by Tucker McClanahan, is a script that reads in the mctal file from MCNP and returns the tally data in a dictionary of numpy arrays for easier analysis in Python.

3.6 Multi-Tier UAS Source Localization

Working in parallel with the Bayesian algorithm described to this point is the design of a novel multi-tier algorithm for aerial search-agent flight-pattern control. Benjamin Lajos Magocs has integrated large area, medium area, and local pinpointing capability into a single algorithm to run collaboratively with the Bayesian processing methods with single aircraft or multi-drone swarming aircrafts.

The large area search tier operates on a predetermined path to identify regions of elevated raw counts and, if applicable, neutrons using a partial integration of energy curves to produce a quasi-gamma/neutron discrimination. Then the medium, or broad area tier, uses raw counts to update the probability field within preset grids, highlighting hot spot locations within the search space. Finally, the small area (i.e. pinpointing) method focuses on high probability locations by means of a Right Angle Turn (RAT) method (Figure 3.4).

This algorithm also utilizes a central data repository for its hot spot and subsequent flight pattern determinations. Mr. Magocs' triple-tier system integrated with Bayesian inference methods is a methodical and effective approach to the problem large region of aerial based source localization.

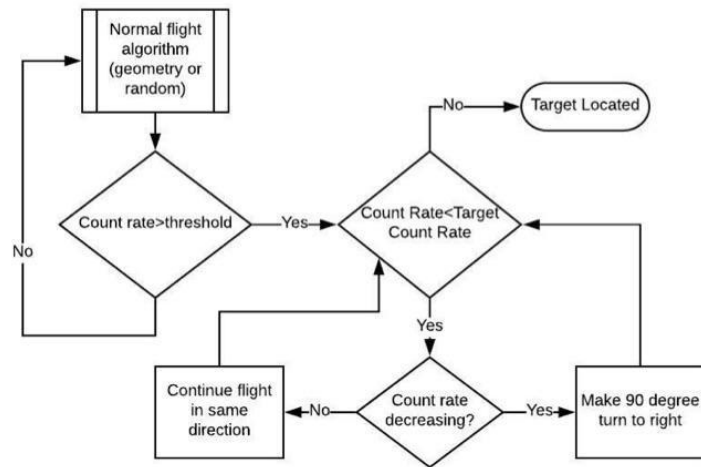


Figure 3.4: Process flow of Right Angle Turn (RAT) localization method [9]

Chapter 4

Results

This chapter will present the results from testing the Bayesian algorithm across multiple simulated scenarios. Single and multi-drone tests will be conducted in a simulated environment with a bare Cs-137 source, and the effectiveness of critical design considerations as well as the implementation of the Bayesian algorithm in the project's multi-tier localization system will be demonstrated.

4.1 Multi-Drone Simulation

To test the multiple input, output, and multi-agent control features of the Bayesian algorithm multiple drones are simulated flying through a virtual space created with a Monte Carlo N-Particle transport code (MCNP6). The MCNP environment is designed to replicate the project's current site for live flight tests, with a bare Cs-137 source placed within the space. The test site is 157 meters in length and 45 meters wide, roughly 1.75 acres.

Drones are created as instantiations of the Drone subclass and each travel three predetermined paths across the space. The code is designed in such a way that n-drones can be instantiated for a search. Three drones were used for this demonstrations as an arbitrary number to demonstrate the multi-agent control. After each length across the area the drones push their collected data to the central data repository to update the posterior hypothesis. The posterior hypothesis is represented as probability densities across the x and y axis. Note that probability densities are related to the probability but are not exact probability values. Thus a higher probability density expresses a greater degree of belief in one possible result over another based on the data currently available.

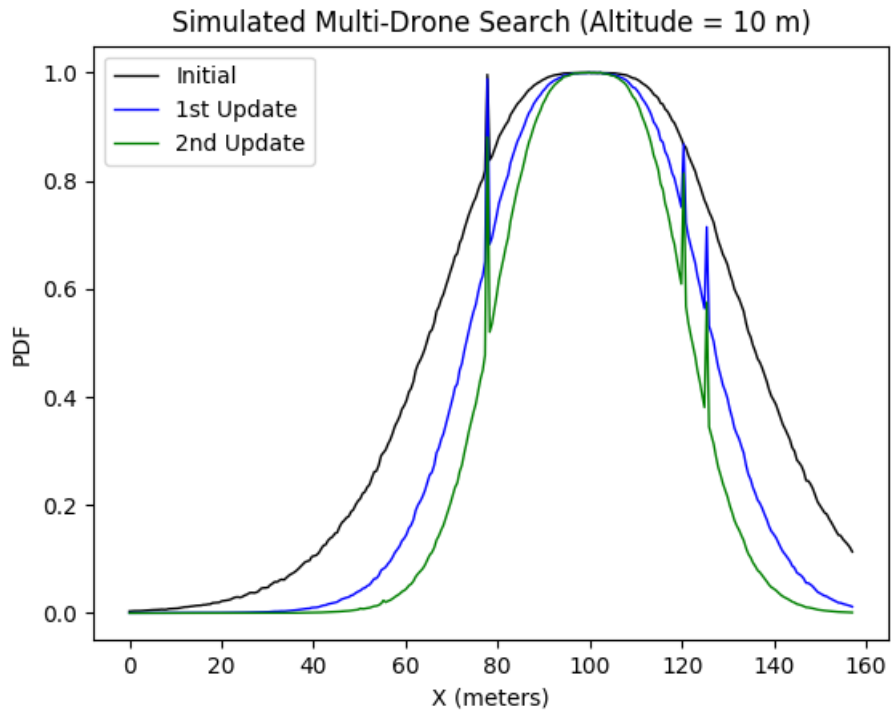


Figure 4.1: X-dimension posterior distributions at search height of 10 meters.

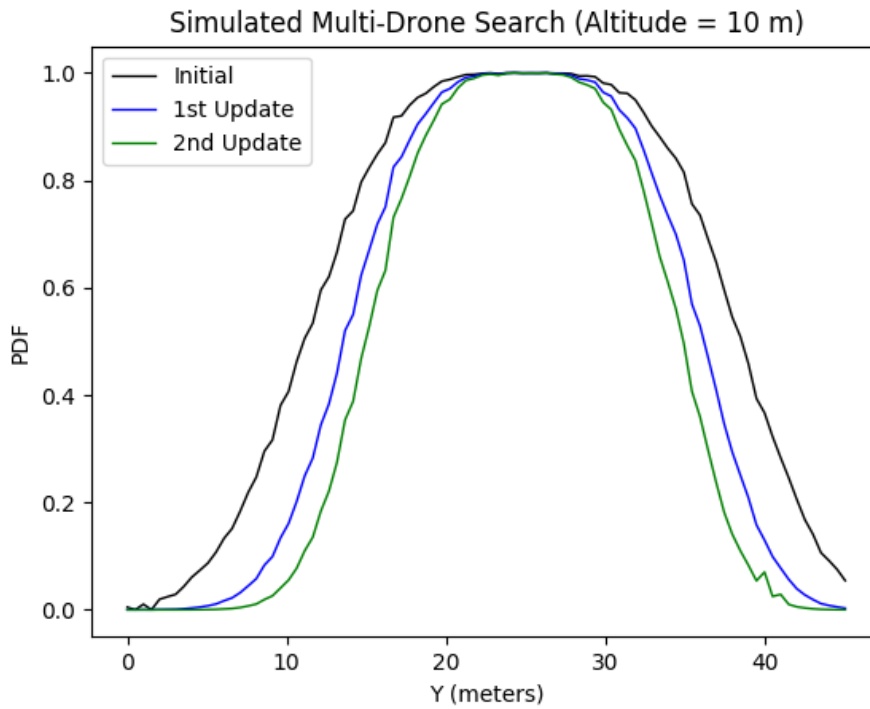


Figure 4.2: Y-dimension posterior distributions at search height of 10 meters.

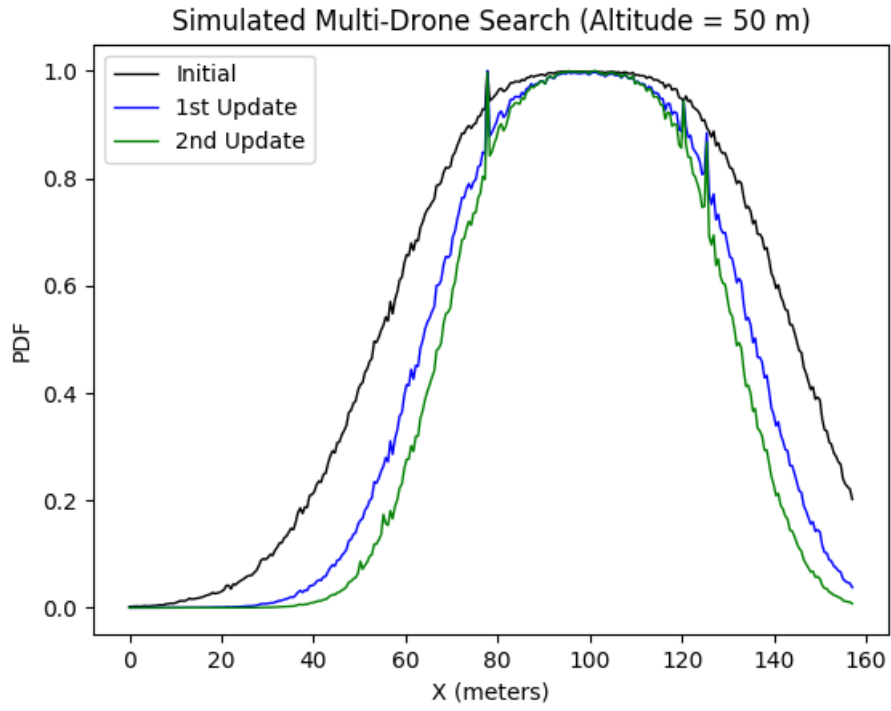


Figure 4.3: X-dimension posterior distributions at search height of 50 meters.

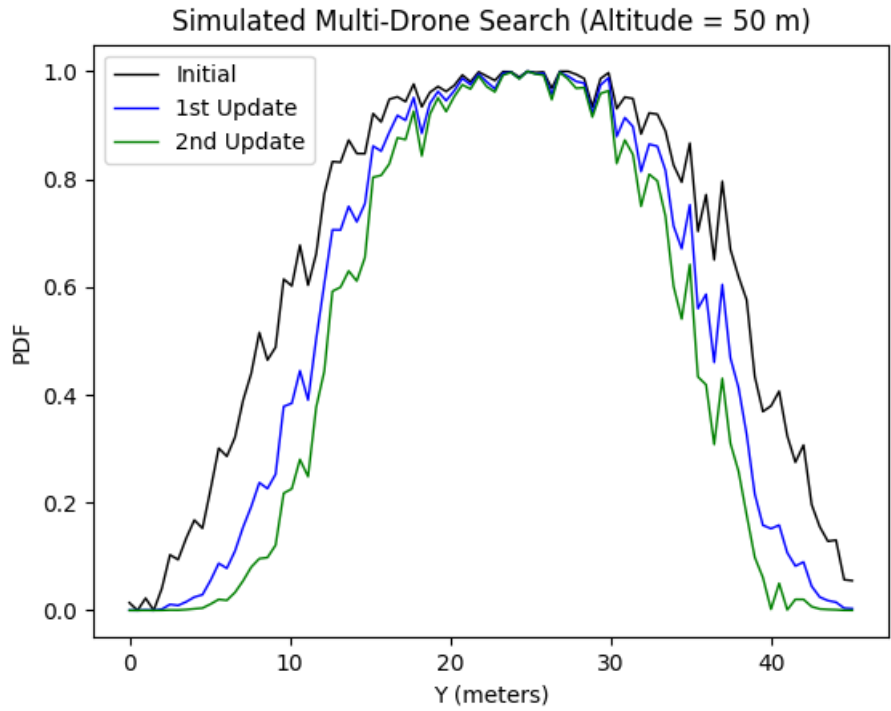


Figure 4.4: Y-dimension posterior distributions at search height of 50 meters.

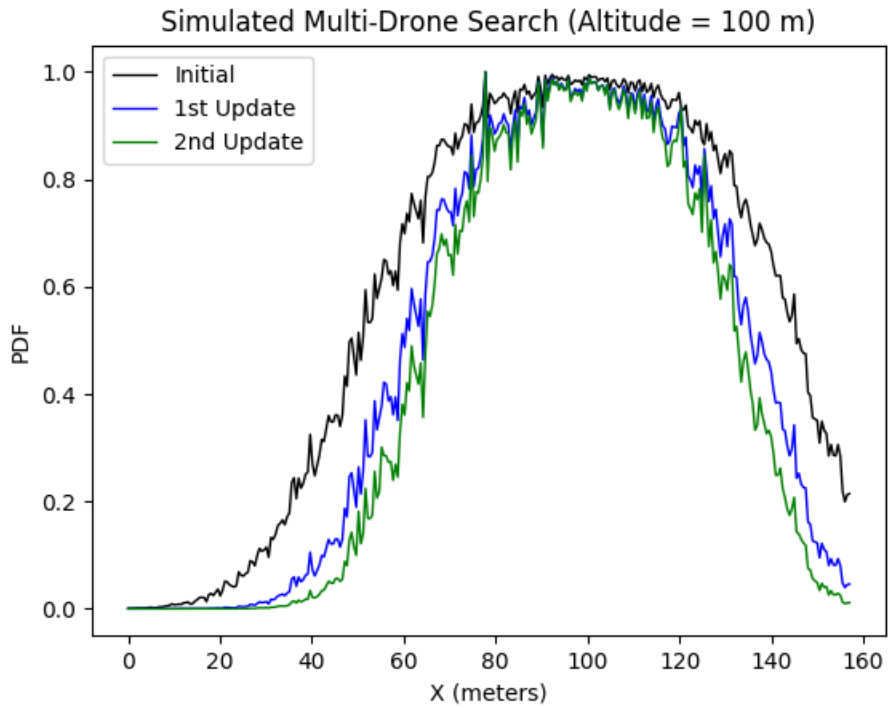


Figure 4.5: X-dimension posterior distributions at search height of 100 meters.

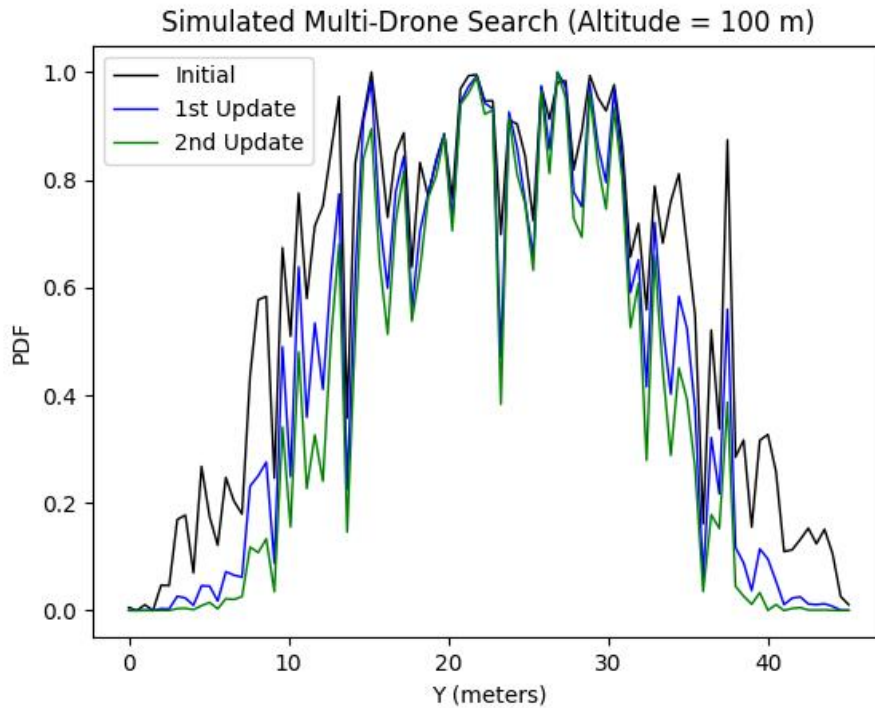


Figure 4.6: Y-dimension posterior distributions at search height of 100 meters.

Figures 4.1-4.6 display the results of the simulated multi-drone search at three different altitudes; 10 meters (Figures 4.1 & 4.2), 50 meters (Figures 4.3 & 4.4), and 100 meters (Figures 4.5 & 4.6).

In each figure the three curves represent the posterior hypothesis at three different points of the search. The black line represents the posterior hypothesis after each drone's initial survey of the search space. The blue line represents the updated posterior hypothesis after the drones fly across the space a second time and the green line shows the resulting posterior after the second update.

Defining an area of high interest, or hotspot, within the search space as the area outlined by probability densities greater than 0.9, the x and y coordinates in Table 4.1 can be extracted from the probability density distributions at each altitude.

Figure 4.7 is a visual approximation of the rendered hot spots from the simulation. The x and y boundaries of the hotspots are returned by the Bayesian algorithm however the visual representation above is not currently an output of the code.

Figures 4.8-4.10 display the results if the same data were to be collected and a single posterior distribution rendered, as opposed to iteratively updating the posterior hypothesis throughout the search.

Table 4.2 shows the defined areas of high-interest from the simulated search without Bayesian updating.

To highlight the efficacy of the Bayesian method the high-interest area sizes for the Bayesian and non-Bayesian searches at various altitudes are compared in Table 4.3. Both tests utilized the same data points for the posterior calculations. By Bayesian methods (i.e. calculating the likelihood of incoming data against the prior likelihood as new information is available) the resulting area of interest was approximately half that of a non-Bayesian approach (single probability density calculation).

Table 4.1: Rendered x and y coordinates for high-interest areas of Bayesian search at various altitudes.

Altitude	y ₁	y ₂	x ₁	x ₂
10 meters	19.5	30.8	88.2	112
50 meters	18.2	31.2	81.4	117
100 meters	17.4	31	77.6	120.8

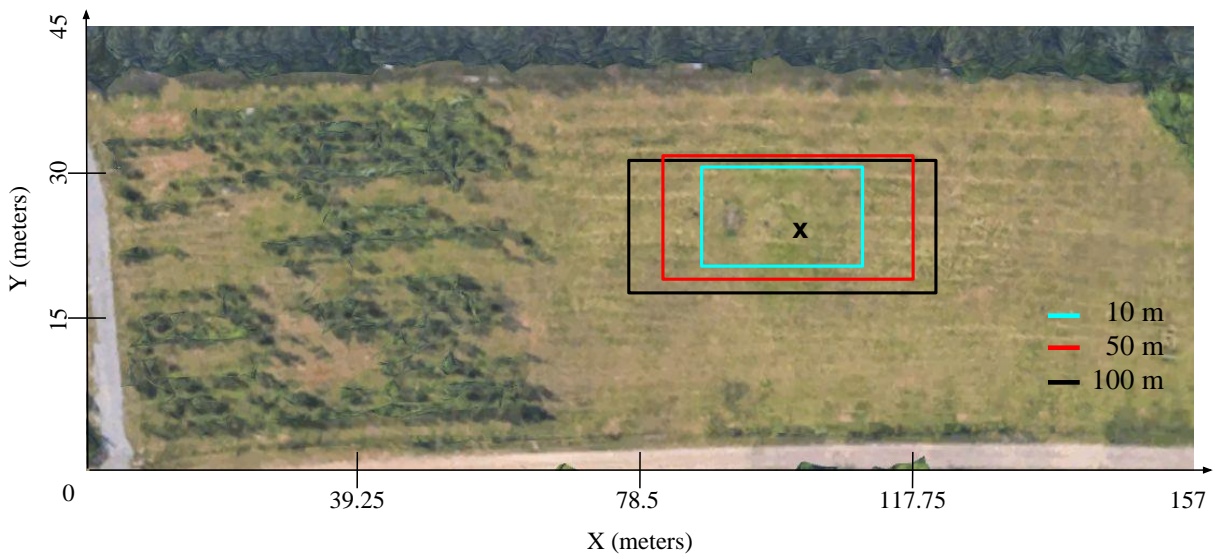


Figure 4.7: Visual representation of high-interest areas from Bayesian search simulation.

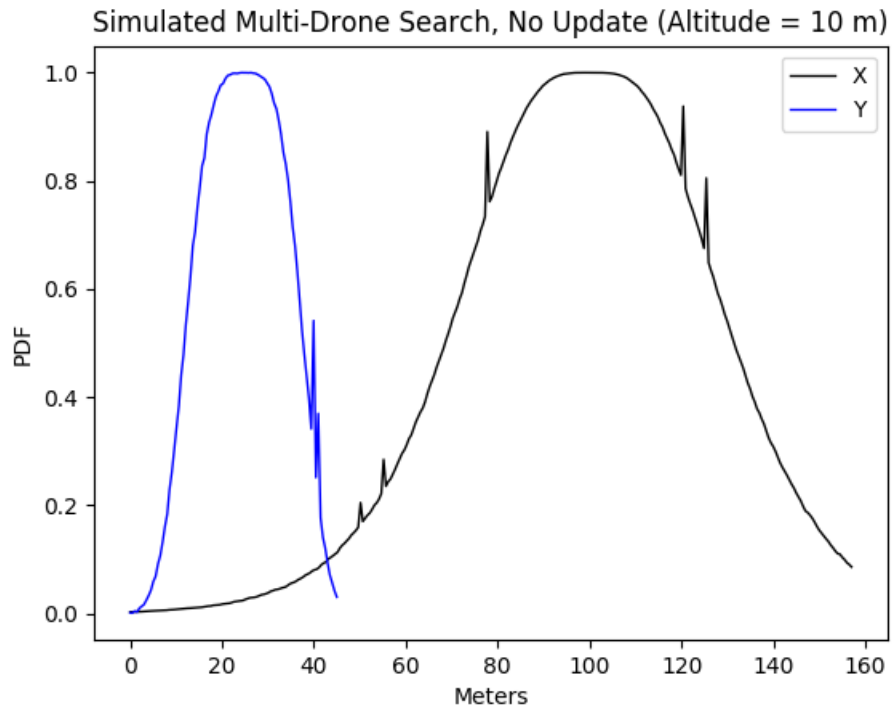


Figure 4.8: Posterior distribution of surveyed area at 10 meters, no updating.

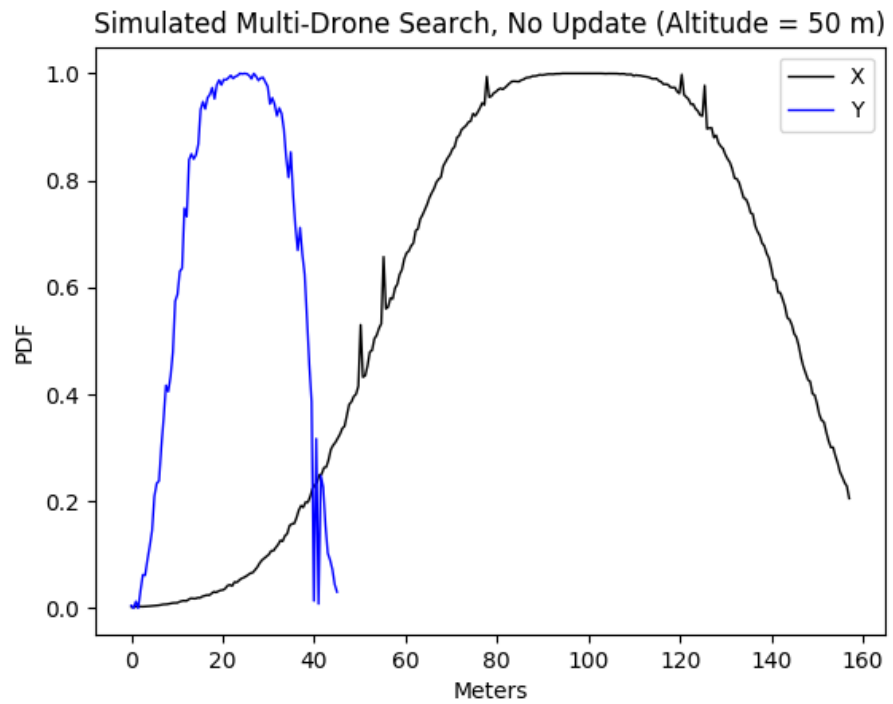


Figure 4.9: Posterior distribution of surveyed area at 50 meters, no updating.

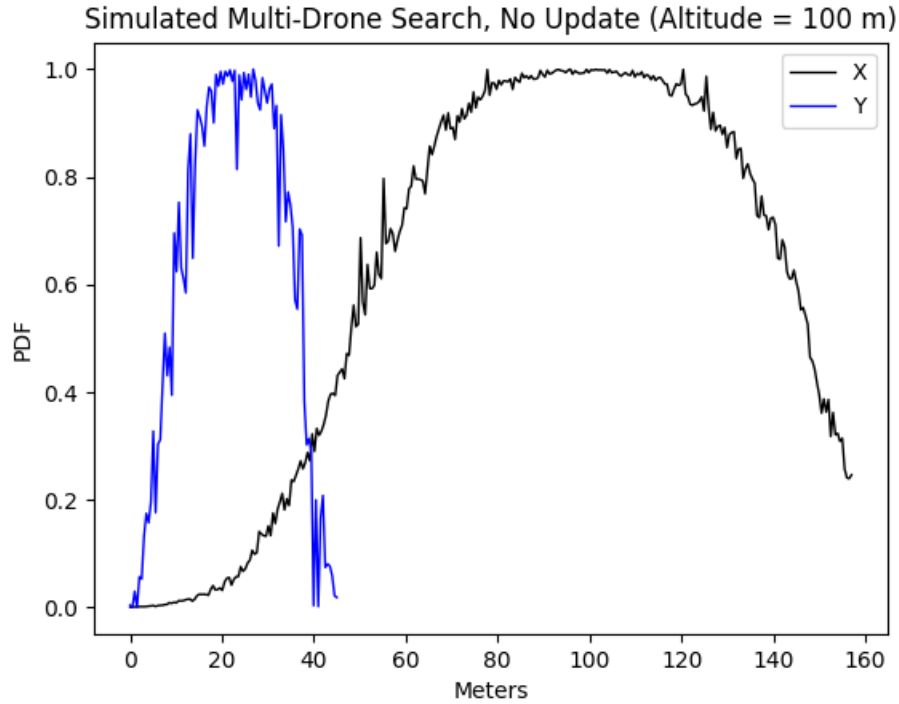


Figure 4.10: Posterior distribution of surveyed area at 100 meters, no updating.

Table 4.2: Rendered x and y coordinates for high-interest areas of non-Bayesian search at various altitudes.

Altitude	y ₁	y ₂	x ₁	x ₂
10 meters	17.0	32.4	84.8	115.8
50 meters	15.0	33.6	72.8	126.0
100 meters	14.8	33.2	67.7	127.1

Table 4.3: Rendered high-interest area sizes of Bayesian versus non-Bayesian tests.

Altitude	Bayesian Search (m ²)	Non-Bayesian Search (m ²)	%-Difference
10 meters	268.9	477.4	77.5
50 meters	462.8	989.5	113.8
100 meters	587.5	1094.7	86.3

4.2 Multi-Tier Bayesian Localization

Benjamin Lajos Magocs is developing a multi-tier algorithm for the flight-pattern control of the aerial search agents throughout the search (see Section 3.6). This section demonstrates how the Bayesian algorithm is integrated as the middle-tier.

Potential hot spots identified by the large area search (tier 1) render waypoints to determine the aircraft's path for the medium area search (tier 2). As the drone travels through the search space, arrays of data are stored containing the drone's latitude, longitude, altitude, as well as the count rate at that point. Figure 4.11 shows the simulated flight path within the tier 2 search.

Figure 4.11 displays the aircraft's path through the search space (black line) as well as the maximum likelihood location from the Bayesian processing methods (blue marker) against the maximum count rate observed (red marker). As the search runs for longer periods of time the maximum likelihood location shifts closer to the region of maximum count rate observed. In this simulation the average latitude and longitude of the two locations is represented by the purple marker. This estimated location is less than 5 meters from the source's true location.

Figure 4.12 displays the measured count rates along the aircraft's flight path (top) and the resulting posterior distribution (bottom) at the end of the tier 2 search. The detection number along the x-axis in Figures 4.12 and 4.13 corresponds to the ordered index of the data array stored by the search agent along its flight path. Each detection number corresponds to a point in space (latitude, longitude, and altitude) which can be indexed within the code. Hotspot locations identified by the Bayesian estimate along with the maximum counts observed are passed to the small area pinpointing tier.

The location of maximum count rate observed by the aircraft is determined by employing a Savitzky-Golay filter to the raw data spectrum. In Figure 4.13 the raw count rate spectrum shows the tallest peak to be around detection number 580. However, the Savitzky-Golay filtered spectrum shows the true maximum count rate to occur closer to the source's true location, at detection instance 475. The convolution method employed by the Savitzky-Golay filter enables larger differentials over shorter distances to be highlighted, creating better distinction the true signal from outliers and background noise

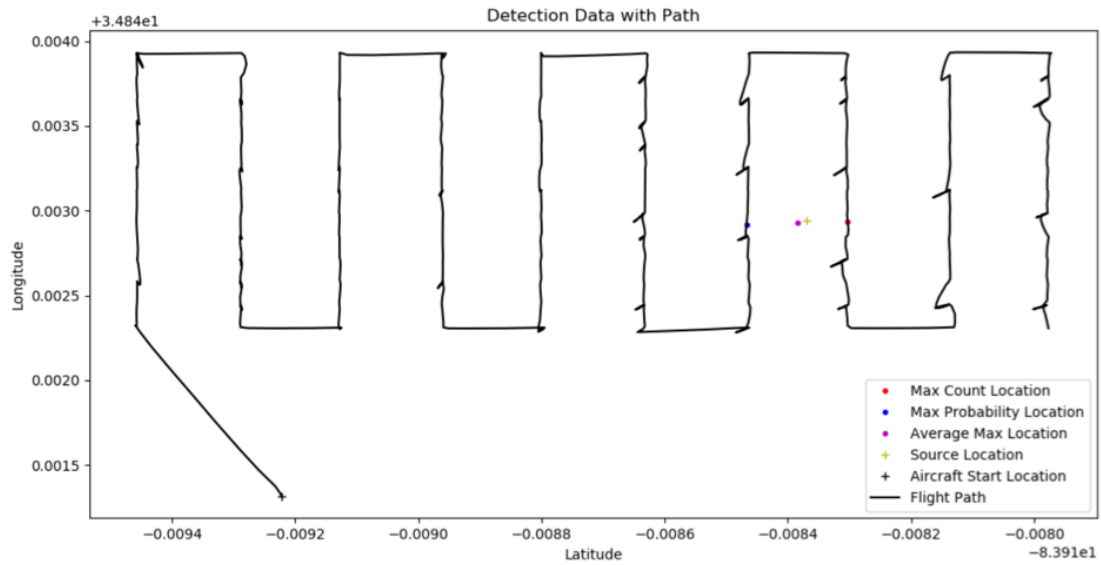


Figure 4.11: Simulated flight path and resulting prediction from tier 2 search [9].

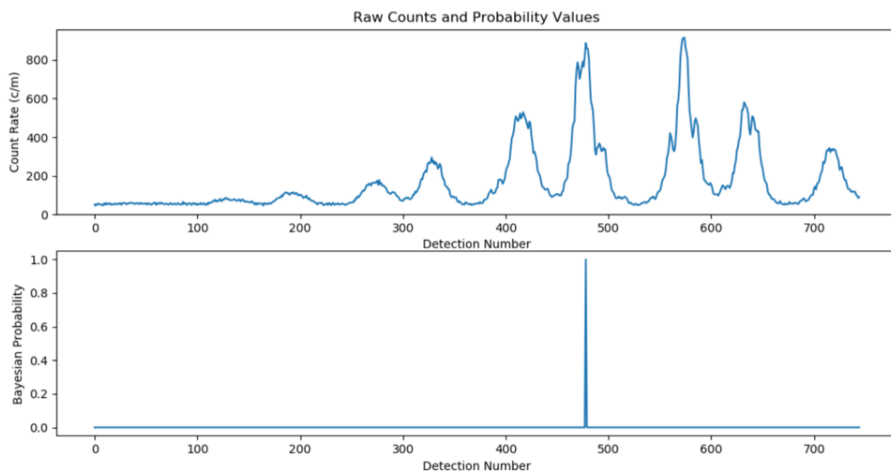


Figure 4.12: Raw counts and posterior distribution at end of tier 2 search [9].

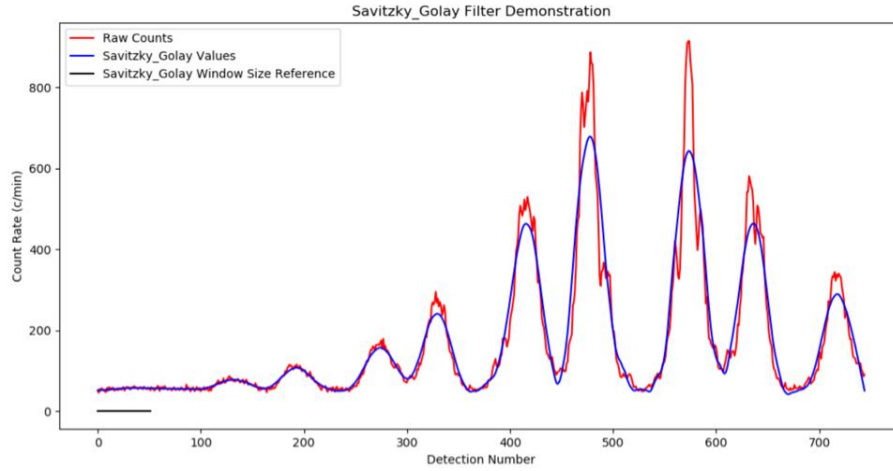


Figure 4.13: Savitzky-Golay filter over raw data spectrum [9].

Chapter 5

Discussion

Nuclear security and nonproliferation efforts rely heavily on proper stewardship of radiological materials as well as the ability to locate and retrieve stolen or missing material. As the amount of nuclear material used in medicine, academic research, and other industrial applications continues to increase so does the amount of material which must be protected and accounted for. Dirty bombs are an effective tool for a potential terrorist attack. Combining small amounts of radioactive material with conventional explosives can contaminate public areas and create widespread anxiety. They are a significant threat to nuclear security and reinforce how critical the ability to locate these lost or stolen radioactive sources is, before they can be used in such a manner.

The SWARM project combines Bayesian inference techniques with the Swarm Intelligence (SI) theory to advance multi-agent aerial source localization methods as a solution to large-area search problems. The Bayesian algorithm presented in this report utilizes a decentralized framework to allow for independent multi-agent control throughout the search. The search agents collect data locally and push to the global data repository when the posterior hypothesis is to be updated. Multithreading capability allows for multiple inputs and outputs at one time as well as for the individual search agents to operate without delaying the response of the main code. Bayesian inference methods are already a proven tool for large area search problems. Applying that tool to an aerial-based search effort and developing a network to handle multiple local search agents each feeding back data to a central repository in order to rapidly locate rogue materials addresses a critical gap in the nuclear security field.

Preliminary simulations have demonstrated the SWARM algorithm's ability to collect and store data locally in the drone's repository until a push to the global repository is requested, update the posterior distribution of the space, and identify areas of interest based on a given probability density threshold.

Figures 4.1-4.6 display the resulting posterior distributions of a simple simulation where multiple search agents survey a field containing a bare Cs-137 source. There are no obstructions and no shielding surrounding the source. Thus, the data is smooth and easy for the drones to

locate the source. Each update calculates the likelihood of the newly obtained data against the previous distribution. In this simulation the updates reduce the width of the posterior distribution, increasing the confidence regarding the source's location. The primary focus of this test was to demonstrate the functionality of the SWARM algorithm's critical components. Future tests will begin to stretch the limits of the code's abilities (i.e. shielded materials, multiple sources, larger search areas). It can be seen in Figures 4.5 and 4.6 that noise plays a significant factor, even in a simulated environment, at 100 meters.

Figure 4.7 shows the effectiveness of the Bayesian algorithm for quickly reducing the area of interest within the search. By setting the threshold at $PDF > 0.9$ the original search space was reduced by over 90% after each drone flew three lengths of the area at an altitude of 100 meters. By contrast, if the same data points were to be collected and processed all at once (i.e. not updating the posterior hypothesis throughout the search) Figures 4.8-4.10 display the posterior PDFs for the x and y coordinates of the search space. The width of these distributions is significantly greater than Figures 4.1-4.6 where, Bayesian update methods process the likelihood of the data against the current hypothesis. Thus, the posterior area of interest for the non-Bayesian search is also greater. Table 4.3 compares the areas of interest rendered by the posterior distributions for the Bayesian and non-Bayesian calculations.

The Bayesian methods of the SWARM code have also been integrated smoothly as the middle tier of Benjamin Lajos Magocs' multi-tier aerial-based source localization algorithm. In simulation the Bayesian code was able to identify a hotspot within 5 meters of the source's true location. This hotspot was then passed to the third and final tier of Mr. Magocs' algorithm.

Effective aerial-based source localization capability is an immediate necessity for locating lost or stolen nuclear materials. The work done in years one and two of the SWARM project has laid the foundation to address this need. The SWARM algorithm has been designed as a simple solution to a complex problem. Year three of the project will take the Bayesian search code beyond simulation to live drone tests. This project shows great promise for being able to address the need for rapid source localization in large, possibly urban environments.

Chapter 6

Future Work

The next step of this project is to apply the Bayesian search algorithm to live flight tests with one, or multiple, of the project's drones. With respect to the code, it is yet to be seen how the analysis methods will fare against more complicated scenarios. The statistical processing methods are intended to be simple and as agnostic as possible so that the application of this code may extend beyond the immediate scope of the SWARM effort. Complications such as shielding of the source, multiple sources, or large urban scenarios where abnormal radiative effects can produce anomalies in the data have not yet been experimented with. When these effects are explored, the efficiency of parametric versus nonparametric density estimations should be compared. Additionally, testing the SWARM code in larger test areas will be interesting to see how effective of a method it would be to feed the resulting hot spots in as a new search space, iteratively narrowing the scope of a large area down to a source(s) location. The class structure of the SWARM code enables this next step to potentially be rather simple. The coordinates of the hotspot could be saved as a class attribute, then called and subsequently overridden each iteration. This will be one of the next steps taken to advance the Bayesian algorithm and continue the effort of designing a powerful multi-agent search code.

Bibliography

- [1] IAEA Incident and Trafficking Database (ITDB). *Incidents of Nuclear and Other Radioactive Material Out of Regulatory Control*. 2016. <http://www-ns.iaea.org/downloads/security/itdb-fact-sheet.pdf>
- [2] McGrayne, Sharon Bertsch. *The Theory That Would Not Die: How Bayes' Rule Cracked the Enigma Code, Hunted down Russian Submarines, and Emerged Triumphant from Two Centuries of Controversy*. Yale University Press, 2012.
- [3] "Nuclear weapons timeline | ICAN." <http://www.icanw.org/the-facts/the-nuclear-age/>. Accessed 4 Oct. 2018.
- [4] "Backgrounder on Dirty Bombs." *United States Nuclear Regulatory Commission*, May 2018, www.nrc.gov/reading-rm/doc-collections/fact-sheets/fs-dirty-bombs.html.
- [5] Shuster, Simon. "Inside the Uranium Underworld: Dark Secrets, Dirty Bombs." *Time*, 6 Apr. 2017.
- [6] L. Kelly, Dana. Smith, Curtis. "Risk Analysis of the Space Shuttle: Pre-Challenger Bayesian Prediction of Failure." (2008).
- [7] Stone, Lawrence D. *The Theory of Optimal Search*. Elsevier, 1975.
- [8] H. Xiao, R. Cui and D. Xu, "A Sampling-Based Bayesian Approach for Cooperative Multiagent Online Search With Resource Constraints," in *IEEE Transactions on Cybernetics*, vol. 48, no. 6, pp. 1773-1785, June 2018.
- [9] Magocs, Lajos, "PADUA Search Algorithm". PhD diss., University of Tennessee, 2019. *In Progress*
- [10] Erin A Miller, Sean M Robinson, Kevin K Anderson, Jonathon D McCall, Amanda M Prinke, Jennifer B Webster, and Carolyn E Seifert. *Adaptively Reevaluated Bayesian*

Localization (ARBL): A novel technique for radiological source localization. Nuclear Instruments and Methods in Physics Research Section A: Accelerators, Spectrometers, Detectors and Associated Equipment, 784:332–338, 2015.

https://ac.els-cdn.com/S0168900215000698/1-s2.0-S0168900215000698-main.pdf?_tid=47ee8ba3-107e-4042-aca8-92f35001250d&acdnat=1545256845_9dc17c79a1ca609c5d414b8fbefa50aa

[11] “Treaty on the Non-Proliferation of Nuclear Weapons (NPT)”. *International Atomic Energy Agency*. <https://www.iaea.org/>. Accessed 4 Oct. 2018.

[12] *Treaty on the Non-Proliferation of Nuclear Weapons*. U.S. -U.K. - S.S.R., etc. <https://www.un.org/disarmament/wmd/nuclear/npt/>. Accessed 4 Oct. 2018.

[13] Wilkerson, Robert Blake, "A Bayesian Approach to Aerial Localization of Radioactive Sources." Master's Thesis, University of Tennessee, 2016. http://trace.tennessee.edu/utk_gradthes/4273

[14] Hall, Howard L. *Semi-Autonomous Wide Area Radiological Measurements (SWARM) Phase II Proposal*. February, 2017.

[15] Willmon, Samuel James, "A Bayesian Approach to Broad-Area Nuclear and Radiological Search Operations." PhD diss., University of Tennessee, 2014. https://trace.tennessee.edu/utk_graddiss/2781

[16] Tsoulfanidis, Nicholas. *Measurement and Detection of Radiation*. Taylor & Francis, 2011.

[17] “Savitzky–Golay Filter.” *Wikipedia*, Wikimedia Foundation, 7 Jan. 2019, en.wikipedia.org/wiki/Savitzky%E2%80%93Golay_filter.

[18] Robert D Penny, Tanya M Crowley, Barbara M Gardner, Myron J Mandell, Yanlin Guo, Eric B Haas, Duane J Knize, Robert A Kuharski, Dale Ranta, Ryan Shyffer, Simon Labov, Karl

Nelson, Brandon Seilhan, and John D Valentine. Improved radiological/nuclear source localization in variable NORM background: An MLEM approach with segmentation data. Nuclear Instruments and Methods in Physics Research Section A: Accelerators, Spectrometers, Detectors and Associated Equipment, 784:319–325, 2015

Vita

Joshua Gurka is from Crofton, MD. In 2013 he graduated from the Key School in Annapolis, MD and continued on to attend the University of Tennessee (UT), Knoxville. He received his Bachelor of Science degree in nuclear engineering in 2017 and remained at UT to pursue his Master's degree in nuclear engineering. After graduating in the spring of 2019 Joshua will attend Officer Candidate School (OCS) in Newport, RI to become a submarine officer in the United States Navy.